de Haas-van Alphen effect in gallium

F. W. Holroyd* and W. R. Datars
Department of Physics, McMaster University, Hamilton, Canada L8S 4M1
(Received 23 November 1977)

The de Haas–van Alphen (dHvA) effect in gallium single crystals has been studied using the low-frequency field-modulation technique with the magnetic field up to 5.7 T parallel to the three principal crystallographic planes. Many dHvA frequencies have been observed and most have been identified using Reed's pseudopotential model of the Fermi surface of Ga although some frequency branches remain unexplained. The large previously unseen eighth-band electron surface has been observed in its entirety and a small seventh-band electron surface has been identified. Frequencies due to the small fifth-band hole surface and many frequencies attributed to the large complex comprising seventh- and eighth-band electron surfaces have been observed. Some of the observed orbits result from magnetic breakdown between the seventh- and eighth-band surfaces. The large multiply connected sixth-band hole surface is expected to have comparatively few extremal orbits according to Reed's model and most of these were observed. In addition, several new frequencies (not explicitly predicted by Reed) are attributed to this surface. Frequencies from some closed Fermi-surface pieces were expanded in terms of spherical harmonics and inverted to yield radii.

I. INTRODUCTION

The band structure and Fermi surface of Ga have been the subject of numerous investigations. A nearly-free-electron (NFE) model was used to explain magnetoresistivity and Hall-effect data.[1] Other experiments showed that the NFE model was hopelessly inadequate, and a slightly better model was calculated by Wood[2] using an augmented-plane-wave method. This involved an *ad hoc* potential which did not greatly change the energy-band structure from that of the NFE model but produced a Fermi surface that was considerably different. In 1969, Reed[3] published a pseudopotential calculation which employed a local semiempirical pseudopotential without spin-orbit coupling. Induced torque[4] and magnetoresistance measurements[5,6] showed that this model gives the correct open-orbit structure. Other previous data also supported this model. The present work was done to test this model further and to provide a complete set of de Haas–van Alphen (dHvA) frequencies for Ga.

There have been previous experiments on the dHvA effect in Ga employing a torsion balance,[7] the modulation method without computerized Fourier analysis,[8] magnetothermal oscillations,[9] oscillations in the uniaxial stress dependence,[10] and magnetoresistance.[11] In the regions in which the data can be compared, there is good qualitative agreement, although quantitative agreement is difficult to determine without tabulated values. However, the present results are much more complete, giving dHvA frequencies of orbits not seen before and showing others over a larger angular range of magnetic field. The interpretation of some of the dHvA frequency branches is also changed using this larger set of experimental data.

II. EXPERIMENTAL METHOD

Single crystals of gallium were grown from oriented seeds using a method similar to that of Yaqub and Cochran.[12] A 2-mm-diam hole was bored crosswise in a 3-mm-diam Kel-F rod. The hole was filled with liquid gallium which was then supercooled and crystallized using the oriented seed. Crystal orientation was changed during the experiment by rotating the rod about its axis using a gear-reduction mechanism accurate at the sample to ± 0.16°. This procedure provided good strain-free crystals with the minimum surface damage by eliminating the necessity of cutting a crystal, cleaning its surface, and holding it with cement. It also minimized strain due to differential thermal contraction since Kel-F and gallium have similar coefficients of thermal expansion. However, this gain was at the cost of some accuracy in crystal alignment. Although the seed was aligned to 0.25°, there was no guarantee that the crystal growth would propagate in a straight line and it was not possible to correct small misalignments because it was fixed in the holder. The only check possible on accurate alignment, therefore, except for gross errors, was self-consistency of the data.

The low-frequency field-modulation technique[8,13] was used to detect the dHvA signal. The modulation frequency was 517 Hz and the maximum field of the superconducting magnet was 5.7 T. Detection was at the second harmonic of the modulation frequency. The data were recorded on magnetic tape and were analyzed using a fast Fourier trans-

form algorithm. In the computer program for the analysis, corrections in amplitude could be made for the Bessel function, present because of the modulation method, the exponential term, the 1/B factor, the hyperbolic sine term, and the temperature variation of amplitude in the dHvA amplitude.[14] These corrections were used to eliminate any false broadening of the frequency response. The data could also be apodized with a triangular window function to decrease the amplitude of side bands.

Data were collected for magnetic field directions in the three principal planes of gallium. The angular mesh was approximately 2.8° for each of the three planes except where a mesh of 1.1° was required for certain frequency branches near symmetry axes. For each magnetic field direction, data were taken as a function of reciprocal field using several dc magnetic field sweep ranges and speeds and suitable modulation field strengths to enhance various frequency branches.

III. EXPERIMENTAL RESULTS

The low and high dHvA frequencies are shown in Figs. 1 and 2, respectively. Frequency branches are labeled *An*, *Bn*, and *Cn*, where *n* is a number from 1 to 20, 22, and 21, respectively. In general, higher values of *n* correlate with higher frequencies. With one exception in Fig. 1, only fundamental frequencies are shown, the harmonics and combinations being suppressed. The frequencies and the relative strengths of the various dHvA oscillations for all orientations are tabulated elsewhere.[15] The experimental dHvA frequencies at symmetry directions are shown in Table I.

The actual orientations of the crystal planes

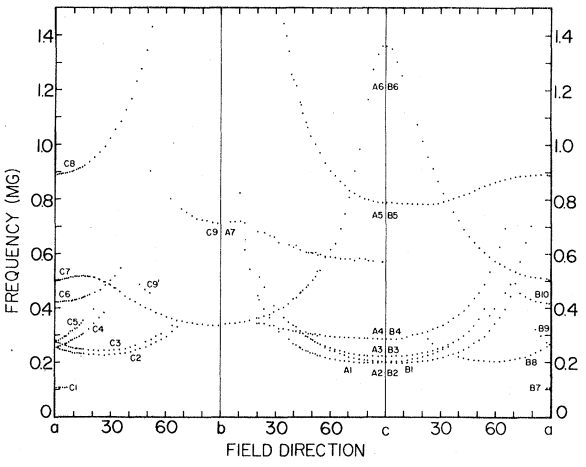

FIG. 1. dHvA frequencies up to 1.5 MG for magnetic field directions in the three principal planes of gallium.

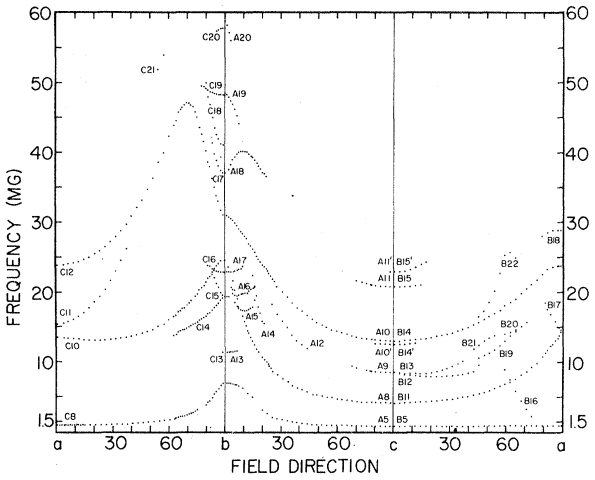

FIG. 2. dHvA frequencies between 1.5 and 60 MG for magnetic field directions in the three principal planes of gallium.

that were studied were determined by noting that, if the crystal had been accurately aligned, branches $C10$ and $C11$ should meet at the frequency at which $B11$ and $B17$ cross at the $\vec{a}$ direction. The separation of $C10$ and $C11$ indicated that the nominal a direction in the ab plane was actually 2.2° toward $\vec{c}$ from $\vec{a}$. Similarly, by comparing $A10$ and $C12$, it was calculated that for the bc plane, the orientation at 90° was actually 0.6° from $\vec{b}$ toward $\vec{a}$. No other inconsistencies in orientation were found.

The above orientational error was the only error that could be taken into account in the analysis. The Fourier transform resolution was approximately ±0.0008 MG for the low frequencies and ±0.02 MG for the intermediate and high frequencies. The sample turning mechanism used to change the orientation of the sample resulted in a positional uncertainty of ±0.16°. An error of ±0.02% in magnetic field readings calibrated by nuclear magnetic and errors at high fields due to magnetic interactions[16] set the error limits of the high and intermediate frequencies at ±0.1 MG and ±0.06 MG, respectively. The error limits of the low frequencies were set at the Fourier transform resolution of ±0.0008 MG.

IV. DISCUSSION

The dHvA frequencies are interpreted in terms of Reed's model[3] of the Fermi surface of Ga shown in Fig. 3. Frequencies which were generated by ellipsoidal or near-ellipsoidal surfaces were studied by plotting inverse frequency squared as a function of $\cos^2\theta$ (henceforth termed a $1/f^2$ plot), which is linear for an ellipsoidal surface. Frequencies predicted by Reed's model at sym-

TABLE I. dHvA frequencies at symmetry directions in this experiment (E) and predicted by Reed's model (T).

Piece	Frequencies (MG) $\bar{H}\parallel\hat{a}$		$\bar{H}\parallel\hat{b}$		$\bar{H}\parallel\hat{c}$	
	E	T	E	T	E	T
7e butterfly (L) (central)	14.5	12.2	37.1	35.9	22.4	21.8
7e butterfly (L) (noncentral)	23.8	22.2	48.1	42.6		
7e butterfly–8e at L (central, MB)			30.9	28.4	13.1	12.7
7e butterfly–8e at L (noncentral, MB)			22.9	21.5		
8e at L	14.5	12.2	24.5	20.9	4.16	3.94
7e near Γ	0.891	0.704	6.94	6.65	0.790	0.843
6h at T	0.508	0.52	0.335	0.346	1.36	1.26
7e between arms		5	0.356	0.705	0.287	0.468
7e at N	0.263	0.22		0.42		0.55
8e at N	0.263	0.22		0.14		0.26
5h at X		0.37			0.223	
6h monster legs ($k_x = 0$)	0.419	0.45				
6h monster arms ($k_z = \frac{1}{2}k_c$)					0.201	0.37
6h double monster (central)			57.7	52	20.8 [a]	21.8
6h monster–5h at X (central, MB)				26.4	12.5 [a]	10.9
6h monster (noncentral)			41.1		8.55 [a]	11.2
unassigned	28.9		19.4			
unassigned			11.4			

[a] Uncertain assignment. MB: magnetic-breakdown orbit.

metry directions are compared with measured frequencies in Table I. The assignment of the frequency branches to this model are shown in Table II.

Frequency branches $A6$, $B6$, and $C7$ are assigned to 6h ellipsoids at T. Deviations from ellipticity as determined by a $1/f^2$ plot correspond to a significant compression near the bc plane and a smaller bulge near the ab plane. These estimates are borne out by the results of the expansion and inversion scheme which will be presented. This is the first study in which the $C8$ and $A5$ branches have been reported in their entirety. The $1/f^2$ plot for $C8$, $A5$, and $B5$ given in Fig. 4 shows significant deviations from ellipticity. The small closed surface generating them is a nearly circular pancake lying in the ac plane with its edges in the $\hat{c}$ direction curved off this plane approximately 10° toward $\hat{b}$. This is approximately the shape of Reed's 7e saucer at Γ.

The above two surfaces are the only two closed surfaces obviously evident in Fig. 1. However, there are two more which have not been identified previously. The first arises from the branches $C9'$, $C9$, $A7$, $A4$, and $B4$. A $1/f^2$ plot identified $A7$ as the second harmonic of $A4$ and $C9$ to be a harmonic since one-half the frequency of $C9$ and $A7$ intersect the b axis at the same frequency. The fundamental frequencies of $C9$ and $A7$ near the b axis were not observed. The important point to note is that $C9'$, $C9$ and $B4$ indicate ellipsoidal tendencies in a $1/f^2$ plot,

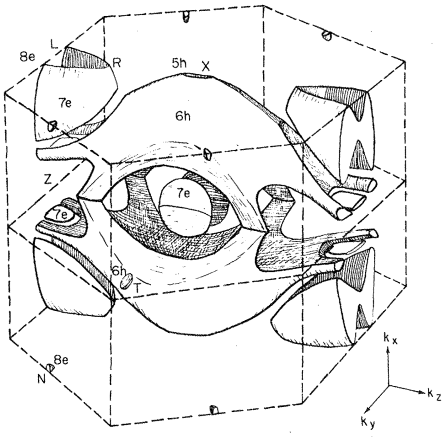

FIG. 3. Drawing of the Fermi surface of gallium based on the calculations of Reed. The pieces of the model Fermi surface in approximate order of decreasing size are the sixth-band hole ($6h$) surface called the monster, the seventh-band electron ($7e$) butterfly surface centered at L, the eigthth-band electron ($8e$) ellipsoid surface inside the butterfly, a pair of $7e$ saucer surfaces displaced slightly from Γ in the $\vec{b}$ direction, a pair of $7e$ pancake surfaces between the monster arms, a pair of sixth-band hole ($6h$) pieces along the ΓT line, a small 5th band hole ($5h$) ellipsoidal surface at X, a small $7e$ surface in the shape of crossed disks at N (not shown) and small $8e$ pieces inside these at N.

whereas $A4$ and $A7$ show that this closed surface must be reasonably flat and thin in the bc plane. This piece is, therefore, matched to the seventh-band electron surface between the monster arms in Reed's model. The frequency predictions of the model for this piece given in Table I are not good because this piece is extremely sensitive to the exact Fermi level. Reed's calculations used a Fermi level of 0.713 Ry; reducing this to 0.710 Ry caused this piece to disappear.

The final piece of Fermi surface which can be termed closed with any reasonable certitude based on the data of Fig. 1 arises from $A3$ and $B3$. They appear to arise from a small nearly ellipsoidal piece of Fermi surface with two nearly equal axes in the $\hat{a}$ and $\hat{b}$ directions and one longer axis in the $\hat{c}$ direction. Only one piece of Reed's model fits this description and that is the fifth-band hole ellipsoidal surface at X. It is also reasonable that no data were observed for this piece in the ab plane since all extremal orbits measured for this piece in this plane must intersect the crystallographic line XRL where the degeneracies existing on the hexagonal face are not lifted by spin-orbit coupling[17] so that electrons cross over to the monster.

Branches $A1$, $A2$, $B1$, and $B2$, which were not distinguished clearly previously,[8-10] are assigned to cross sections of the arms of the monster because they exist over the angular range expected for the arms and the frequencies of the branches increase as the field is rotated away from the $\hat{c}$-axis. Reed's model predicts a frequency of 0.37 MG for the arms with $B11$ $\hat{c}$ which is considerably larger than that observed. Branches $C2$-5, $B8$, and $B9$ are assigned to the $7e$ butterfly surface at N or to the $8e$ ellipsoid nested inside the butterfly. The separation of $C2$ and $C3$ and also $C4$ and $C5$ due to the orientational error described in the previous section shows the sensitivity of the pieces to small orientation errors and that there is degeneracy for the field exactly in the a-b plane.

We turn now to a consideration of the high frequencies shown in Fig. 2. Only $C12$, $A9$-11, and $B12$-15 can be said to have been seen previously with any degree of accuracy.[8] It is immediately obvious from Fig. 2 that the high frequencies are extremely complex. These high frequencies are due primarily to the ellipsoid-butterfly combination at L but some are also due to the monster surface as shown in Table II. Explanation of only some of the assignments will be given here.

For the branches $C10$-$A8$-$B11$, $A8$ and $B11$ can be fitted to an ellipsoid quite well but $C10$ does not fit an ellipsoid prediction. The 14.4 MG frequency at the $\hat{a}$ axis splits into two if the field is rotated away from $\hat{a}$. If the field is rotated more than 9° from $\hat{a}$ toward $\hat{c}$ then $B17$ disappears as expected for orbits on the butterfly. This splitting and the disappearance of $B17$ at the proper angle added to the proximity of the predictions of Reed's model for $8e$ at L to the measured frequencies shown in Table I is enough to confirm the assignment of $C10$-$A8$-$B11$ to $8e$ ellipsoids at L. Branches $C12$, $C10$, and $B14$ have been assigned to the butterfly by Reed. However, since $C11$ and $C17$ are due to central orbits on the butterfly, with minimal cross-sectional area, $C12$ and $B14$ near $\hat{a}$ are due to noncentral maximum orbits on the butterfly.

The model predicts that a frequency of 12.7 MG should be observable with the magnetic field parallel to $\hat{c}$ due to a two-winged butterfly orbit caused by magnetic breakdown. It is easily seen that if the field is rotated from $\hat{c}$ to $\hat{a}$ this magnetic-breakdown orbit transforms continuously into the noncentral maximum orbit within approximately 4° of $\hat{a}$. Since $B14$ has been identified as being due to the noncentral maximum orbit for the field near $\hat{a}$, it must also be due to the two-winged butterfly orbit caused by magnetic breakdown for the field near $\hat{c}$. This also identifies $A10$ near $\hat{c}$ since both have a frequency of 13.1 MG at $\hat{c}$. The

TABLE II. Observed frequency assignments in Reed's model.

A	1	monster arm: $k_y > 0$	*B* 1	monster arm: $k_x < 0$	*C* 1	
	2	monster arm: $k_y > 0$	2	monster arm: $k_x < 0$	2	$7e$–$8e$ at N
	3	$5h$ at X	3	$5h$ at X	3	$7e$–$8e$ at N
	4	$7e$ between arms	4	$7e$ between arms	4	$7e$–$8e$ at N
	5	$7e$ near Γ	5	$7e$ near Γ	5	$7e$–$8e$ at N
	6	$6h$ at T	6	$6h$ at T	6	monster leg
	7	$7e$ between arms (2nd harmonic)	7		7	$6h$ at T
	8	$8e$ at L	8	$7e$–$8e$ at N	8	$7e$ near Γ
	9	monster [a]	9	$7e$–$8e$ at N	9	$7e$ between arms (2nd harmonic)
	10	$8e$ at L–2-wing butterfly (MB, central)	10	monster leg	9′	$7e$ between arms
	10′	monster–$5h$ at X (MB)	11	$8e$ at L	10	$8e$ at L
	11	double monster	12	monster [a]	11	butterfly (central)
	11′	4-wing butterfly	13	monster [a]	12	butterfly (a: noncentral, b: central, MB to $8e$ at L)
	12	monster	14	butterfly (a: noncentral, c: central, 2-wing MB to $8e$ at L)	13	
	13		14′	monster–$5h$ at X (MB)	14	
	14		15	double monster [a]	15	
	15		15′	4-wing butterfly	16	butterfly–$8e$ at L (MB, noncentral)
	16		16		17	butterfly (central)
	17	butterfly–$8e$ at L (MB, noncentral)	17	butterfly (central)	18	monster side (noncentral)
	18	butterfly (central	18		19	butterfly (noncentral)
	19	butterfly (noncentral)	19		20	double monster
	20	double monster	20		21	
			21			
			22			

[a] Uncertain assignment. MB: magnetic-breakdown orbit.

frequency due to the four-winged butterfly orbit for $\vec{B} \parallel \hat{c}$ is then expected to be twice the two-winged butterfly frequency less the ellipsoid frequency, or 22.1 MG. This is close to the 22.4 MG frequency actually observed for $A11'$ and $B15'$.

The region near $\hat{b}$ is the most complicated as there are fully a dozen high frequencies at or near $\hat{b}$. Some have already been explained and $C12$ and $A8$ have been identified with the butterfly. However, for $C12$, the maximum noncentral cross section due to magnetic breakdown transforms continuously at $\theta_{ab} = 39°$ into the central breakdown orbit for $\vec{B} \parallel \hat{b}$. Since the ellipsoid has a maximum central orbit with a frequency of 24.5 MG and the butterfly and ellipsoid have a central breakdown orbit with a frequency of 30.9 MG, the central minimum orbit of the butterfly is expected to have a frequency of 37.2 MG. $C17$ has a frequency of 32.1 MG and so $C17$ and $C18$ are assigned to the central minimum orbit of the butterfly. If the field is rotated from $\hat{b}$ toward $\hat{a}$, the frequency of this orbit is expected to increase sharply, as is seen for $C17$. Of the highest frequencies for $\vec{B} \parallel \hat{b}$, $C20$ and $A20$ at approximately 58 MG are matched with the double monster orbit which is expected to have a frequency of 52 MG and to exist over a very small angular range. Of the remaining data, $C16$ and $A17$ have been assigned correctly by Reed to the noncentral magnetic breakdown orbit between $8e$ at L and the butterfly.

For the field between $\hat{b}$ and $\hat{c}$, only one addi-

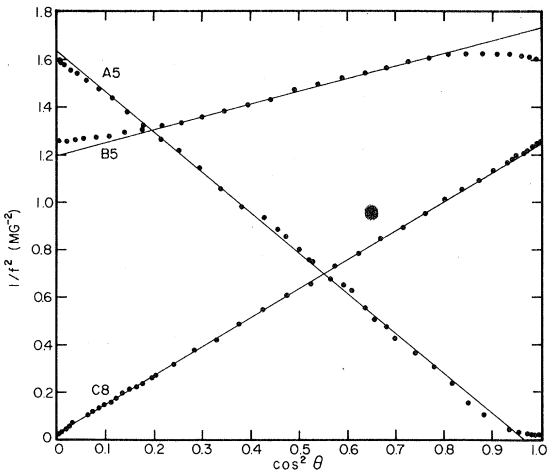

FIG. 4. $1/f^2$ plot for frequency branches $C8$–$A5$–$B5$ attributed to the seventh-band electron surface near Γ.

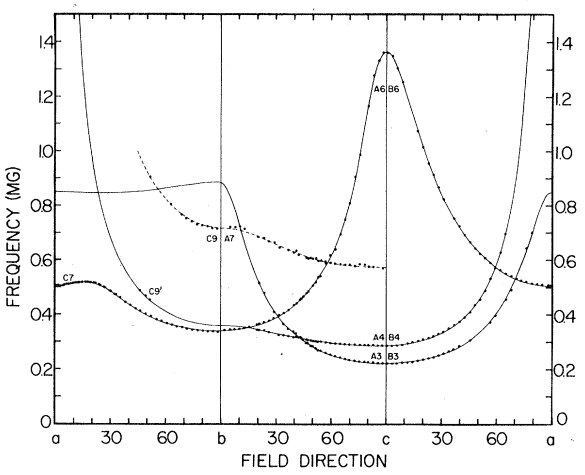

FIG. 5. Spherical harmonic expansion of several dHvA frequency branches of Ga. The solid lines are the least-squares fit to the branches and the dotted line is the second harmonic of one of the branches.

tional frequency ($A12$) was observed. This was observed without comment by Goldstein and Foner and was not identified by Reed. This study presents better data for this branch but will have to leave it unidentified except for the comment that it is more likely to be on the monster than on the butterfly whose orbits are reasonably well known.

An expansion and inversion scheme[18] was used by expanding the Fermi-surface areas in terms of spherical harmonics

$$A(\vec{\xi}) = \sum_{lm} a_{lm} Y_l^m(\vec{\xi}) \tag{1}$$

and simultaneously expanding the square of the radius

$$\rho^2(\vec{\epsilon}) = \sum_{l'm} b_{l'm'} Y_{l'}^{m'}(\epsilon), \tag{2}$$

where $\vec{\xi}$ and $\vec{\epsilon}$ are directions in three dimensions and Y_l^m are spherical harmonics. The coefficients are related by

$$b_{lm} = a_{lm}/\pi P_l(0). \tag{3}$$

The restrictions on this scheme are that the surface must be closed with a center of inversion symmetry [since $P_l(0) = 0$ for l odd], and the radius vector of the surface from the point of inversion symmetry must be single valued in all directions. Thus, some of the closed pieces of the Fermi surface without an inversion center, although having several mirror planes, are not suitable for inversion and were not inverted. Reference 15 gives the expansion coefficients of a spherical harmonic least-squares approximation to the data of four closed surfaces. The fit of the expansion to the frequencies of the three smaller pieces is shown in Fig. 5.

V. SUMMARY

The de Haas—van Alphen effect in Ga single crystals has been studied using the low-frequency field-modulation technique with the magnetic field, up to 5.7 T, parallel to the three principal crystallographic planes. Frequencies due to small sixth-band hole and seventh-band electron surfaces previously observed by Goldstein and Foner[8] over part of their expected range of magnetic field direction have been extended to show closed pieces of Fermi surface. Many new frequencies have also been observed and most have been identified using Reed's pseudopotential model of the Fermi surface of Ga. The large previously unseen eighth-band electron surface has been observed in its entirety and a small seventh-band electron surface, previously observed in part of one plane but not identified correctly, has now been identified. Frequencies due to the small fifth-band hole surface and many frequencies attributed to the large complex comprising seventh- and eighth-band electron surfaces have been observed. The large multiply connected sixth-band hole surface is expected to have comparatively few extremal orbits according to Reed's model and most of these were observed. In addition, several new frequencies not explicitly predicted by Reed are attributed to this surface. Thus, Reed's pseudopotential model is a reasonable model of the Fermi surface of Ga. It has the proper connectivity and contains pieces of approximately the correct size, shape, and placement. Some of these sur-

faces or parts of surface are more easily verifiable experimentally than others and the easily verifiable parts fit the data reasonably well. Comparison of the measured and predicted frequencies for symmetry directions is given in Table I. The model can be used to explain 75% of the observed frequency branches in this study, including most major branches. However, there are still many unexplained data. This includes one frequency (branch $C14$) in the *ab* plane which was the dominant observed frequency throughout most of its approximately 30° range of existence. The explanation of these data may lie in a thorough numerical analysis of Reed's model for field directions in the principal crystallographic planes. But, it is more likely that the solution of this problem lies in using Reed's model as the basis for a better band-structure calculation.

ACKNOWLEDGMENTS

We wish to thank W. A. Reed for making available many of the unpublished details of his calculations and R. J. Douglas for constructing a model of the Fermi surface. One of us (W.R.D.) extends thanks to Professor F. Koch for the hospitality of his group at the Technical University of Munich during the writing of this paper. The research was supported by a grant from the National Research Council of Canada.

---

*Present address: Dept. of Physics, University of Toronto, Ontario, Toronto, Canada.

[1]W. A. Reed and J. A. Marcus, Phys. Rev. 126, 1298 (1962).
[2]J. H. Wood, Phys. Rev. 146, 432 (1966).
[3]W. A. Reed, Phys. Rev. 188, 1184 (1969).
[4]J. R. Cook and W. R. Datars, Phys. Rev. B 1, 1415 (1970).
[5]J. R. Cook and W. R. Datars, Can. J. Phys. 48, 302 (1970).
[6]J. C. Kimball and R. W. Stark, Phys. Rev. B 4, 1786 (1971).
[7]J. H. Condon, Bull. Am. Phys. Soc. 9, 239 (1964).
[8]A. Goldstein and S. Foner, Phys. Rev. 146, 442 (1966).
[9]P. Goy, A. Goldstein, D. Langenberg, and J. C. Picard, Phys. Lett. A 25, 324 (1967).
[10]R. Griessen, H. Krugmann, and H. R. Ott, Phys. Rev. B 10, 1160 (1974).
[11]R. L. Brown and C. B. Friedberg, Phys. Rev. B 15, 3817 (1977).
[12]M. Yaqub and J. F. Cochran, Phys. Rev. 137, 1182 (1965).
[13]R. G. Poulsen, J. S. Moss, and W. R. Datars, Phys. Rev. B 3, 3107 (1971).
[14]A. V. Gold, *Solid State Physics, The Simon Fraser University Lectures, Vol.* 1, *Electrons in Metals*, edited by J. F. Cochran and R. R. Haering (Gordon and Breach, New York, 1967), pp. 39—126.
[15]F. W. Holroyd, Ph.D. thesis (McMaster University, 1976) (unpublished).
[16]D. Shoenberg, Philos. Trans. R. Soc. Lond. A 255, 85 (1962).
[17]G. F. Koster, Phys. Rev. 127, 2044 (1962).
[18]F. M. Mueller, Phys. Rev. 148, 636 (1966).